

Engineering of a Novel Ruthenium Sensitizer and Its Application in Dye-Sensitized Solar Cells for Conversion of Sunlight into Electricity

C. Klein,[†] Md. K. Nazeeruddin,^{*†} P. Liska,[†] Davide Di Censo,[†] N. Hirata,[‡] E. Palomares,^{‡§} J. R. Durrant,[‡] and M. Grätzel[†]

Laboratory for Photonics and Interfaces, Institute of Chemical Sciences and Engineering, School of Basic Sciences, Swiss Federal Institute of Technology, CH-1015 Lausanne, Switzerland, Centre for Electronic Materials and Device, Department of Chemistry, Imperial College London, Exhibition Road, SW7 2AZ London, U.K., and Institut de Ciència Molecular (IcMol), Universitat de Valencia, 46100-Burjassot, Valencia, Spain

Received August 27, 2004

A novel ligand 4,4'-bis(carboxyvinyl)-2,2'-bipyridine (L) and its ruthenium(II) complex [Ru(II)L₂(NCS)₂] (**K8**) were synthesized and characterized by analytical, spectroscopic, and electrochemical techniques. The performance of the **K8** complex as a charge transfer photosensitizer in nanocrystalline TiO₂ based solar cells was studied. When the **K8** complex anchored onto a nanocrystalline TiO₂ film, we achieved very efficient sensitization yielding 77 ± 5% incident photon-to-current efficiencies (IPCE) in the visible region using an electrolyte consisting of 0.6 M methyl-*N*-butyl imidazolium iodide, 0.05 M iodine, 0.05 M LiI, and 0.5 M 4-*tert*-butylpyridine in a 50/50 (v/v) mixture of valeronitrile and acetonitrile. Under standard AM 1.5 sunlight, the complex **K8** gave a short circuit photocurrent density of 18 ± 0.5 mA/cm², and the open circuit voltage was 640 ± 50 mV with fill factor of 0.75 ± 0.05, corresponding to an overall conversion efficiency of 8.64 ± 0.5%.

Dye sensitized solar cells are currently attracting widespread interest for the conversion of sunlight into electricity because of their low cost and high efficiency.^{1–7} In these cells, dye is one of the key components for high power conversion efficiencies. The pioneering studies on dye

sensitized nanocrystalline TiO₂ films using *cis*-dithiocyanatobis(4,4'-dicarboxylic acid-2,2'-bipyridine)ruthenium(II) (**N3**) is a paradigm in this field. In spite of this, the main drawback of this sensitizer is the lack of absorption in the red region of the visible spectrum and also the relatively low molar extinction coefficient.⁸ Several groups have tried to overcome these shortcomings without significant success.^{9–12} Molecular engineering of ruthenium complexes for TiO₂-based solar cells presents a challenging task as several stringent requirements have to be fulfilled by the sensitizer which are very difficult to be met simultaneously, including absorbing all the visible light and functioning as an efficient charge-transfer sensitizer. For example, the lowest unoccupied molecular orbitals (LUMO) and the highest occupied molecular orbitals (HOMO) have to be maintained at levels where photoinduced electron transfer into the TiO₂ conduction band and regeneration of the dye by iodide can take place at practically 100% yield. We report here a study in which we have maintained these conditions and at the same time have succeeded in fine-tuning the spectral properties of ruthenium polypyridyl complexes by designing at the molecular level a novel ligand, 4,4'-bis(carboxyvinyl)-2,2'-bipyridine. Our research focused on increasing the optical extinction coefficient of sensitizers, so that dye solar cells could be made thinner and thus more efficient because of reduced transport losses in the nanoporous environment. In this Communication, we report synthesis and characterization of a ruthenium sensitizer using the novel ligand and its application in dye-sensitized solar cell.

* To whom correspondence should be addressed. E-mail: MdKhaja.Nazeeruddin@epfl.ch.

[†] Swiss Federal Institute of Technology.

[‡] Imperial College London.

[§] Universitat de Valencia.

- Grätzel, M. *Nature* **2001**, *414*, 338.
- Nakade, S.; Saito, Y.; Kubo, W.; Kitamura, T.; Wada, Y.; Yanagida, S. *J. Phys. Chem. B* **2003**, *107*, 8607.
- Palomares, E.; Clifford, J. N.; Haque, S. A.; Lutz, T.; Durrant, J. R. *J. Am. Ceram. Soc.* **2003**, *125*, 475.
- Hara, K.; Sato, T.; Katoh, R.; Furube, A.; Ohga, Y.; Shinpo, A.; Suga, S.; Sayama, K.; Sugihara, H.; Arakawa, H. *J. Phys. Chem. B* **2003**, *107*, 597.
- Benkstein, K. D.; Kopidakis, N.; van de Lagemaat, J.; Frank, A. J. *J. Phys. Chem. B* **2003**, *107*, 7759.
- Qiu, F. L.; Fisher, A. C.; Walker, A. B.; Petecr, L. M. *Electrochem. Commun.* **2003**, *5*, 711–716.
- He, J.; Benko, G.; Korodi, F.; Polivka, T.; Lomoth, R.; Åkermark, B.; Sun, L.; Hagfeldt, A.; Sundstrom, V. *J. Am. Chem. Soc.* **2002**, *124*, 4922.

- Nazeeruddin, M. K.; Kay, A.; Rödicio, I.; Humphry-Baker, R.; Muller, E.; Liska, P.; Vlachopoulos, N.; Grätzel, M. *J. Am. Chem. Soc.* **1993**, *115*, 6382.
- Yanagida, M.; Yamaguchi, T.; Kurashige, M.; Hara, K.; Katoh, R.; Sugihara, H.; Arakawa, H. *Inorg. Chem.* **2003**, *42*, 7921.
- Sauvé, G.; Cass, M. E.; Doig, S. J.; Laueremann, I.; Pomykal, K.; Lewis, N. S. *J. Phys. Chem. B* **2000**, *104*, 3488.
- Argazzi, R.; Bignozzi, C. A.; Heimer, T. A.; Castellano, F. N.; Meyer, G. J. *Inorg. Chem.* **1994**, *33*, 5741.
- Heimer, T. A.; Heilweil, E. J.; Bignozzi, C. A.; Meyer, G. J. *J. Phys. Chem. A* **2000**, *104*, 4256.

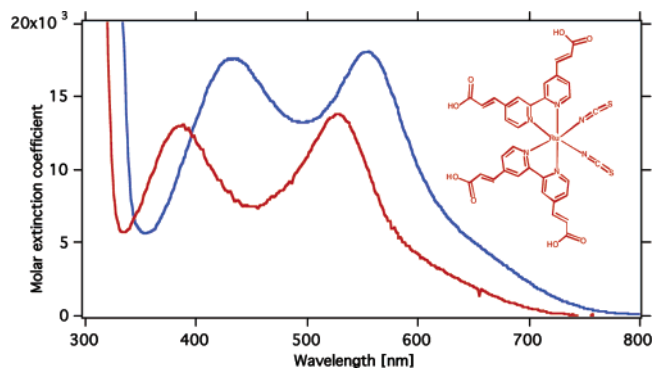


Figure 1. UV-vis absorption spectrum of **K8** (blue line, λ_{max} 555 nm, ϵ 18000 $\text{M}^{-1} \text{cm}^{-1}$) and **N3** (red line λ_{max} 535 nm, ϵ 13600 $\text{M}^{-1} \text{cm}^{-1}$) measured in DMF.

Figure 1 shows the structure of the 4,4'-bis(carboxyvinyl)-2,2'-bipyridine ligand and its ruthenium complex [RuL₂(NCS)₂], **K8**. The ligand 4,4'-bis(carboxyvinyl)-2,2'-bipyridine is synthesized in two steps, and its ruthenium complex is prepared in a one pot synthesis starting from 4,4'-bis(carboxyvinyl)-2,2'-bipyridine and dichloro(*p*-cymene)ruthenium(II) dimer in DMF for 8 h (see the Supporting Information for details).

The absorption spectrum of the **K8** sensitizer is dominated by metal to ligand charge transfer transitions (MLCT) and shows MLCT bands in the visible region at 555 and 439 nm. There are two high-energy bands at 312 and 326 nm due to ligand π - π^* charge transfer transitions. A comparison of UV-vis spectra of the **K8** and the **N3** complexes is shown in Figure 1. The **K8** complex's lowest energy MLCT band is red shifted 20 nm and the molar extinction coefficient increased by 30% when compared to the standard **N3** sensitizer. When the **K8** complex is excited within the MLCT absorption band at 298 K in an air-equilibrated DMF solution, it exhibits a luminescence maximum at 830 nm and a lifetime of 18 (\pm 1) ns. Under similar conditions, the **N3** sensitizer shows an emission maxima at 800 nm with an excited state lifetime of 40 ns (see Figure 2S in Supporting Information). The red shift of the emission maxima of the **K8** complex compared to the standard **N3** sensitizer is consistent with the red shift in the lowest energy MLCT absorption maxima of the **K8** sensitizer.

The ¹H and ¹³C NMR spectra of the **K8** complex measured in DMSO-*d*₆ solution are consistent with the structure (see the Supporting Information). The complex **K8** in solution shows (10) peaks in the aromatic region corresponding to two different pyridyl ring and vinyl protons in which two pyridine rings are trans to the NCS ligands and the remaining two are trans to each other. The proton coupling constant data of the vinyl protons (15.94 and 16.04 Hz) confirm that they are in a trans configuration. The proton decoupled carbon-13 NMR spectrum of complex **K8** in the aromatic region shows 17 peaks. The carbon-13 data are particularly useful in the **K8** complex for determining whether the NCS ligand has N or S bonded coordination. The presence of peak at 134.4 ppm clearly indicates that the NCS coordination to the ruthenium center is through the nitrogen.¹³ The ATR-FTIR spectra measured as a solid sample show a strong and intense absorption at 2097 cm^{-1} that is due to the N-

coordinated $\nu(\text{CN})$. This band is approximately 3.5 times more intense than the band at 800 cm^{-1} , due to $\nu(\text{CS})$. The band at 1701 cm^{-1} is assigned to the C=O stretching of carboxy groups. The four bands at 1608, 1540, 1472, and 1418 cm^{-1} are due to the ring stretching modes of the ligand. The IR bands at 1635 and 972 cm^{-1} are due to characteristic C=C and trans-C-H, respectively, of 4,4'-bis(carboxyvinyl)-2,2'-bipyridine.

The oxidation and reduction potential data of the **K8** complex were obtained using a glassy carbon electrode in DMF solvent with 0.1 M tetrabutylammonium perchlorate. Upon scanning to positive potentials, a quasireversible couple at $E_{1/2} = 0.35$ V versus Fc (ferrocene/ferricenium) with a separation of 0.09 V between the anodic to the cathodic peak was observed due to the Ru^{II/III} couple. The ruthenium oxidation potential in complex **K8** is shifted cathodically by 0.05 V, compared to the **N3** couple. The difference (0.05 V) in the oxidation potential of complex **K8** compared to that of **N3** is due to the donor influence of 4,4'-bis(carboxyvinyl)-2,2'-bipyridine when compared to 4,4'-bis(carboxy)-2,2'-bipyridine. The two reversible waves at $E_{1/2} = -1.83$ and -2.18 V versus Fc are assigned to the reduction of 4,4'-bis(carboxyvinyl)-2,2'-bipyridine.

The excited state oxidation potential of a sensitizer plays an important role in the electron transfer process, which an approximate value can be extracted from the ground state oxidation couple and the zero-zero excitation energy $E(0-0)$ according to eq 1.¹⁴ The $E(0-0)$ energy (1.69 eV) was extracted from the high energy side of corrected emission spectra where the intensity is 10% of the peak intensity. The excited oxidation potential of the **K8** complex is -0.89 V versus SCE, which is sufficiently more negative than the TiO₂ conduction band.¹⁵

$$E(\text{S}^+/\text{S}^*) = E(\text{S}^+/\text{S}) - E(0-0) \quad (1)$$

Pulsed optical excitation of the **K8** sensitizer adsorbed onto nonscattering nanocrystalline TiO₂ films resulted in a long-lived optical absorption transient, as shown in Figure 2. The optical transient exhibited a pronounced absorption maximum at 775 nm, assigned by comparison with the **N3** dye, to an LMCT transition of the **K8** cation species, and consistent with efficient electron injection from the **K8** excited state into the TiO₂ electrode. The optical transient is long-lived, with a decay half time of 200 μs , assigned to charge recombination of the dye cation with TiO₂ electrons.

For photoelectrochemical device fabrication, TiO₂ anatase nanoparticles of 15 nm were prepared by hydrolysis of titanium(IV)isopropoxide as described before.¹⁶ Nanocrystalline TiO₂ thin films of 12 μm thickness were deposited onto transparent conducting glass by screen printing. These films were dried at 150 $^\circ\text{C}$ for 20 min, and then, a 3 μm

(13) Nazeeruddin, M. K.; Zakeeruddin, S. M.; Humphry-Baker, R.; Gorelsky, S. I.; Lever, A. B. P.; Grätzel, M. *Coord. Chem. Rev.* **2000**, *208*, 213.

(14) Caspar, J. V.; Westmoreland, T. D.; Allen, G. H.; Bradley, P. G.; Meyer, T. J.; Woodruff, W. H. *J. Am. Ceram. Soc.* **1984**, *106*, 3492.

(15) Liu, G.; Jaegermann, W.; He, J.; Sundström, V.; Sun, L. *J. Phys. Chem. B* **2002**, *106*, 5814.

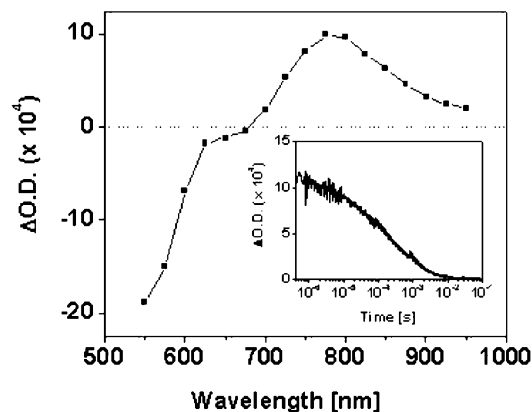


Figure 2. Transient absorption data for 4 μm thick TiO_2 film sensitized with **K8** complex and covered in propylene ethylene carbonate. The transient spectrum was recorded at 100 μs after pulsed excitation at 525 nm, and assigned to the **K8** dye cation/ TiO_2 (e^-) state resulting from photoinduced electron injection. The inset shows the transient absorption data decay dynamics at 800 nm, assigned to charge recombination. All experimental details as reported previously.¹⁷

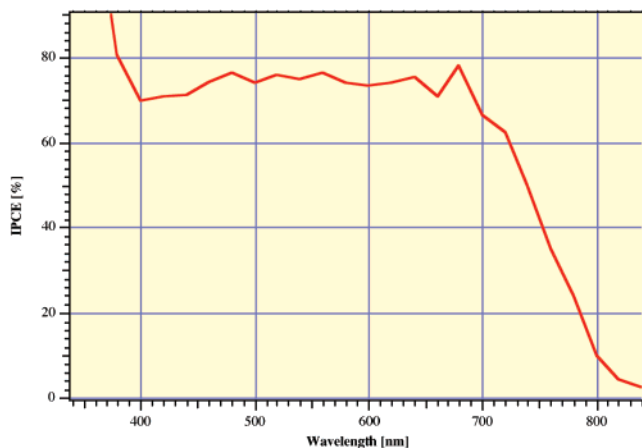


Figure 3. Photocurrent action spectrum obtained with the **K8** complex attached to a nanocrystalline TiO_2 film. The incident photon to current conversion efficiency is plotted as a function of the wavelength of the exciting light. The electrolyte composition was 0.6 M methyl-*N*-butyl imidazolium iodide, 0.05 M iodine, 0.05 M LiI, and 0.5 M *tert*-butylpyridine in a 50:50 (v/v) mixture of valeronitrile and acetonitrile.

thick layer of 400 nm TiO_2 particles (400 nm particles were obtained from CCI, Japan) was deposited again using a screen printing method. The double layered films were sintered at 500 $^\circ\text{C}$ for 20 min, which were then further treated with TiCl_4 as described before.¹⁶ Finally, the electrodes were heated at 500 $^\circ\text{C}$ for 20 min and allowed to cool to 50 $^\circ\text{C}$ before dipping into the dye solution (3×10^{-4} M in 1:1 acetonitrile and *tert*-butyl alcohol).

The photocurrent action spectra obtained with a sandwich cell using an electrolyte having composition of 0.6 M methyl-*N*-butyl imidazolium iodide, 0.05 M iodine, 0.05 M LiI, and 0.5 M *tert*-butylpyridine in 50/50 (v/v) mixture of valeronitrile and acetonitrile is shown in Figure 3. The photocurrent action spectra of the **K8** sensitizer show broad features

covering a large part of the visible spectrum. The incident monochromatic photon-to-current conversion efficiency (IPCE) is plotted as a function of excitation wavelength, showing in the plateau region 77%. Strikingly, the incident monochromatic photon-to-current conversion efficiency even at 700 nm gives a value of 66%. From the overlap integral of this curve, one measures a short circuit photocurrent density of 18.1 mA/cm^2 . In agreement with this measurement under standard global AM 1.5 solar conditions, the cell gave a photocurrent density of 18 ± 0.5 mA/cm^2 , 640 ± 50 mV open circuit potential, and 0.75 fill factor yielding 8.64% efficiency. The significant effect asserted by the ligand containing extended conjugation is evident from the IPCE spectrum in the red region.

The excellent efficiency of the **K8** dye results from its strong optical light absorbance across the visible spectrum. Optical absorbance data from nonscattering TiO_2 films for both the **K8** and **N3** dyes indicated that the **K8** sensitizer resulted in the indistinguishable dye loading per film unit area as compared with the **N3** dye. Similarly, the recombination dynamics for the **K8** dye cation were observed to be indistinguishable from those for the **N3** dye. This latter observation is particularly striking and indicates that the insertion of the vinyl moiety in the binding ligand does not reduce significantly the electronic coupling between the dye cation and the TiO_2 electrode, consistent with the unsaturated nature of this moiety. The electron injection yield, monitored by the magnitude of the photoinduced absorption signal at 1000 nm assigned to TiO_2 electron absorbance, was, however, observed to be 10–20% lower for the **K8** dye relative to **N3**. This observation is consistent with the slightly lower saturated IPCE values for **K8** relative to **N3**, although this effect is balanced by the improved red absorbance of the **K8** dye, resulting in comparable photocurrent generation efficiencies under AM1.5 illumination.

In conclusion, we have successfully tuned the HOMO and the LUMO levels of the ruthenium sensitizer that show an enhanced spectral response and an increased molar extinction coefficient yielding close to an 8.7% efficient cell. To our knowledge, this class of sensitizers has not been previously reported, and this finding opens the way to designing more efficient panchromatic sensitizers that absorb all the visible light including that in the near-IR region by further modification of the ligand architecture, which will improve notably power conversion efficiencies of dye-sensitized solar cells.

Acknowledgment. We acknowledge financial support of this work by the Swiss Federal Office for Energy (OFEN), U.S. Air Force Research Office under Contract F61775-00-C0003, NANOMAX (Contract ENK6-CT-2001-00575 of the fifth RTD framework program by EU and funded by OFES, Bern), and Marie Curie Fellowship Contract HPMF-CT-2002-01744 (for E.P.). We thank Dr. Robin Humphry-Baker for his time and helpful discussions.

Supporting Information Available: Synthesis and analytical and spectroscopic data of the **K8** complex. This material is available free of charge via the Internet at <http://pubs.acs.org> IC048810P

(16) Nazeeruddin, M. K.; Péchy, P.; Renouard, T.; Zakeeruddin, S. M.; Humphry-Baker, R.; Comte, P.; Liska, P.; Cevey, L.; Costa, E.; Shklover, V.; Spiccia, L.; Deacon, G. B.; Bignozzi, C. A.; Grätzel, M. *J. Am. Chem. Soc.* **2001**, *123*, 1613.

(17) Hirata, N.; Lagref, J. J.; Palomares, E. J.; Durrant, J. R.; Nazeeruddin, M. K.; Grätzel, M.; Di Censo, D. *Chem. Eur. J.* **2004**, *10* (3), 595.